

Optical probing of the temperature transients during pulsed-laser induced boiling of liquids

Hee K. Park and Costas P. Grigoropoulos

Department of Mechanical Engineering, University of California, Berkeley, California 94720

Chie C. Poon and Andrew C. Tam^{a)}

IBM Almaden Research Center, 650 Harry Road, San Jose, California 95120-6099

(Received 14 September 1995; accepted for publication 24 November 1995)

The thermodynamics of the rapid boiling of a liquid on a solid surface heated by an excimer laser pulse is studied experimentally. The dynamics of bubble nucleation, growth, and collapse is detected by probing the optical specular reflectance. The transient temperature field is measured by monitoring the reflectance of a thin film with calibrated optical properties. The metastability behavior of the liquid and the criterion for the liquid-vapor phase transition in nanosecond time scale are obtained for the pressure from 1 atmosphere to 3.3 MPa. © 1996 American Institute of Physics. [S0003-6951(96)04805-X]

The interaction of a laser beam with liquids provides important practical applications. The explosive boiling of liquids induced by a short-pulsed laser beam is utilized in laser cleaning of microcontaminants¹ and medical laser treatment.² Short-pulsed laser-induced nucleation and cavitation in a biological tissue produces a sharp incision with minimal injury for accurate surgical operation. The physics of superheated liquids above boiling point and phase transitions has been sought for a better control of such applications. There have been efforts to understand the dynamics of the rapid boiling of liquids on an absorbing solid surface heated by short-pulsed laser irradiation.³ However, no real-time measurement of the surface temperature during the boiling has been made, although the surface temperature is one of the most important parameters in heterogeneous nucleation where the interface serves as the nucleation site. Furthermore, thermodynamic considerations such as the degree of superheat on a liquid-vapor phase transition in nanosecond time scale have never been addressed. Disturbances by bubbles near the solid surface and the relatively low-temperature rise have prohibited the precise detection of surface temperature. Recently, it has been demonstrated that probing the transient optical transmission or reflectance is a fast and reliable method to monitor the development of the temperature field.⁴⁻⁶ In this work, the photothermal reflectance probe has been successfully implemented for the first time to measure the transient temperature during the nanosecond-pulsed laser-induced boiling.

The experimental setup is shown in Fig. 1. The liquid is contained in a pressure cell. The pressure can be varied by applying compressed nitrogen (0.1–3.3 MPa). The liquids tested are water and methanol, which are transparent to the KrF excimer laser heating beam ($\lambda=248$ nm, pulse width=16 ns FWHM). The solid sample has three layers as shown in the inset. The top layer is an UV absorbing film (chromium). The intermediate layer is a thin-film optical temperature sensor whose optical properties vary with tem-

perature. The bottom layer is a transparent quartz substrate. The temperature is probed via the photothermal reflectance of the intermediate layer, i.e., the optical sensor, irradiated from the backside. In this letter, the backside refers to the quartz side. The front side refers to the chromium film side on which nucleation takes place. Polycrystalline silicon (*p*-Si) is selected as the optical temperature sensor. The thickness of the top Cr layer is chosen to be greater than the optical penetration depth (0.01 μm at 248 nm) to prevent the direct heating of the *p*-Si layer by the excimer laser. Thus, the sample is composed of a 0.15 μm thick Cr film and 0.35 μm thick *p*-Si film deposited on a 500 μm thick fused quartz substrate. Both surfaces of the sample are probed with cw lasers. Two probe lasers and the excimer laser beam are shown in Fig. 1. Since the Cr film has no intrinsic thermorefectance effect, any change in the front-side reflectance is ascribed to the formation of bubbles. Therefore, the bubble nucleation behavior and the temperature can be derived independently.

The photothermal reflectivity from the backside of the sample is characterized by a static experiment to obtain the optical properties of quartz substrate and *p*-Si film. The tem-

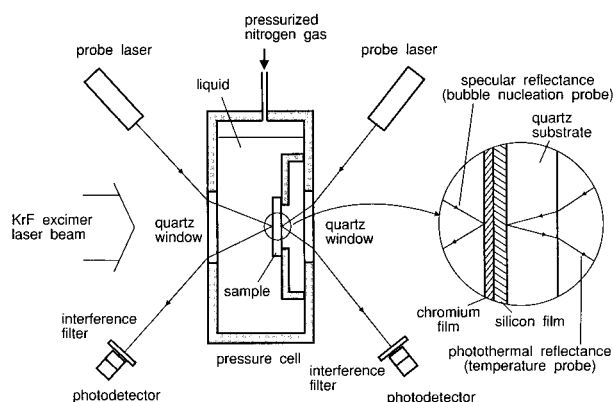


FIG. 1. Schematic of the experimental setup. The probe lasers are a HeNe laser ($\lambda=632.8$ nm) for photothermal reflectance at the backside and an Ar⁺ laser ($\lambda=488$ nm) for specular reflectance monitor at the front side.

^{a)}Electronic mail: actam@almaden.ibm.com

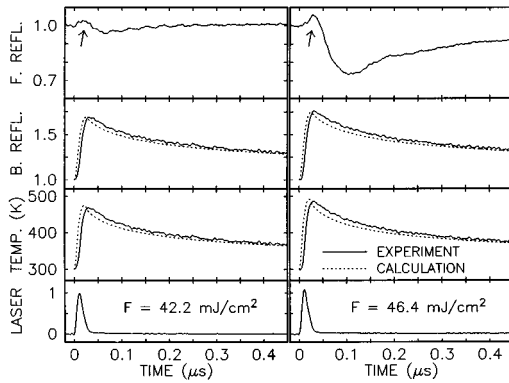


FIG. 2. The experimentally obtained reflectance curves (solid lines) are shown in the top panel (front side reflectance) and the second panel (back-side reflectance) for water at atmospheric pressure. The dotted lines are calculated transient reflectivity response (the second panel) and surface temperature (the third panel). The converted surface temperature traces from the measured reflectances are also shown (solid line in the third panel). The bottom panel shows the excimer laser pulses, $F=42.2 \text{ mJ/cm}^2$ (left-hand side column) and 46.4 mJ/cm^2 (right-hand side column).

perature profile is modeled by a one-dimensional heat diffusion equation. The detailed procedures on the static reflectivity calibration and the temperature modeling appear elsewhere.^{6,7}

Figure 2 shows the results of the transient temperature measurement and bubble growth monitor for the water/chromium interface at two excimer laser fluences. The bubble growth behavior can be observed from the front-side reflectance signal. As bubbles form and grow on the surface, the specular reflectance shows distinct transients, as seen in the top panels. The reflectance increase (marked by arrows in the top panels in Fig. 2) is caused by a thin layer of small bubbles.³ The trailing decrease is due to scattering losses caused by enlarged bubbles. Finally, the slow recovery is due to random bubble collapse. At the lower excimer laser fluence, the front-side reflectance signal (top of the left-hand side column) shows a slight change, indicating the chromium/liquid interface is near the nucleation threshold. The transient temperature measurement is performed simultaneously to understand its relationship with the bubble growth behavior. The second row panels show the experimental photothermal reflectance curve (solid line) and the theoretical response (dotted line). The reflectance signals are normalized to the initial value, i.e., the reflectance at $t=0$ at which time the excimer laser is triggered. It is seen that the modeling result closely follows the experimental curve. The measured and calculated evolutions of surface temperature are compared in the third panels. The experimental surface temperature traces are obtained by deconvoluting the measured reflectance signals based on the calculated spatial temperature profile.⁷ The precision of the temperature measurement can be demonstrated as follows. At the fluence $F=42.2 \text{ mJ/cm}^2$, the measured and calculated maximum surface temperatures are 466 and 476 K, respectively. The difference is within the experimental error. At this condition the measured degree of superheat with respect to the normal boiling temperature at atmospheric pressure is 93 K. A similar measurement for methanol yields the maximum temperature of 430

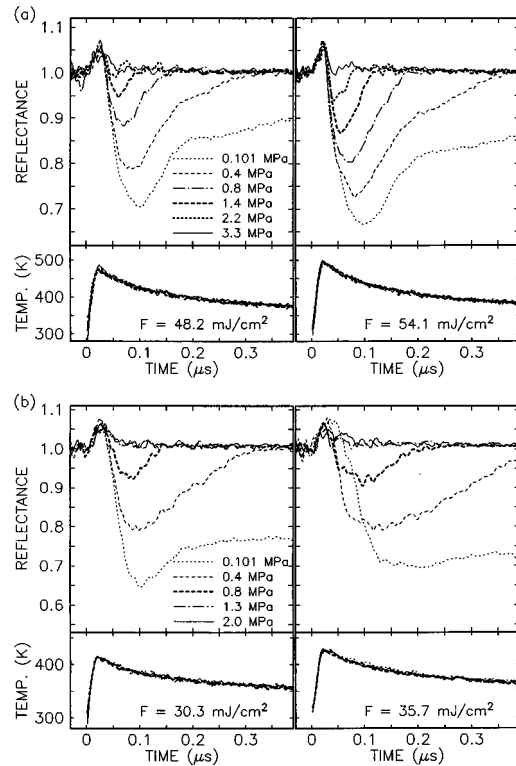


FIG. 3. Specular reflectance signals and measured surface temperature transients at various pressure for (a) water and (b) methanol at a fixed excimer laser fluence. The probe beam is s -polarized Ar^+ laser ($\lambda=488 \text{ nm}$, angle of incidence $\phi=10.5^\circ$).

K at the threshold and therefore, the degree of superheat of 90 K at atmospheric pressure. It is noted that the nucleation starts instantaneously as the surface temperature exceeds the boiling temperature. The nucleation consequently modifies the front-side reflectance. For instance, the first noticeable change in the front-side reflectance at $F=46.4 \text{ mJ/cm}^2$ is detected at $t=13 \text{ ns}$. At this moment, the measured surface temperature is 389 K, only 16 K above the boiling point. For all the conditions tested, this trend remains true. It is therefore concluded that the degree of superheat required for the formation of embryos (microscopic nucleation centers) is significantly lower than that for the formation of bubbles. This effect is observed only by simultaneously monitoring time-resolved bubble growth and surface temperature. Based on this observation, the dynamics of bubble growth can be understood as follows: embryos are nucleated as soon as the surface reaches the boiling condition (nucleation threshold). Bubbles can grow in size if sufficient heat is supplied from the surface. When their radii exceed the limit $R=\lambda/2\pi n$, i.e., about $0.06 \mu\text{m}$ (wavelength $\lambda=488 \text{ nm}$ and refractive index $n=1.34$), scattering losses become much more appreciable and consequently the specular reflectance decreases. From the temperature measurements, such growth takes place only if the surface temperature is about 100 K above the boiling temperature for water and methanol at atmospheric pressure (threshold for the onset of bubble growth). It is noted that the heterogeneous nucleation can be catastrophic according to the measured degree of superheat values, as in the case of homogeneous nucleation.^{8,9}

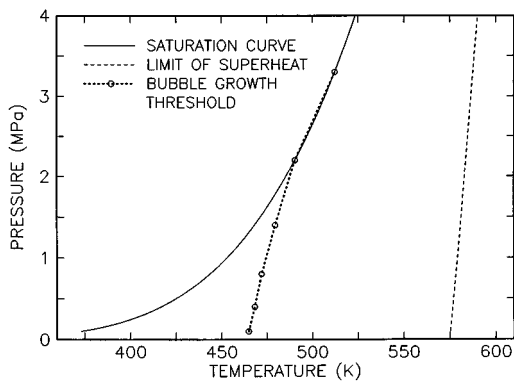


FIG. 4. The bubble-growth threshold temperature and liquid pressure are identified as symbols (○) and connecting dotted lines in p - T diagram for water.

Bubble growth monitoring and transient temperature measurement are also performed at various liquid pressures. The dependence of the front-side reflectance signal on the pressure at a fixed excimer laser fluence is shown in Figs. 3(a) for water and 3(b) for methanol. The initial rise of front-side reflectance, occurring during the nucleation of embryos and when their radius $\ll \lambda/2\pi n$, i.e., when Rayleigh scattering is predominant,³ is nearly insensitive to the liquid pressure because surface tension force dominates. However, at pressures beyond 2.2 MPa, the magnitude of initial rise decreases, as can be seen from the case of water at $F=48.2$ mJ/cm². As bubbles grow in size, scattering in the Mie regime causes a subsequent drop in front-side reflectance. The amplitude of the reflectance drop is proportional to the total scattering cross section of bubbles which is a function of bubble radius and number density.¹⁰ It is observed that the amplitude of the reflectance drop decreases with pressure increase, which indicates a smaller volume of bubbles at a higher pressure. It is also noted that bubble growth and collapse rates are nearly independent of ambient pressure in the pressure range studied. The fact that a smaller total volume of bubbles is produced at higher pressures could be explained by lesser degrees of superheat. The measurements show that the maximum surface temperature is independent of pressure at a constant excimer laser fluence. For the case of water at $F=54.1$ mJ/cm² [Fig. 3(a)], the peak surface temperatures are measured to be around 496 K while the boiling points increase from 373 K at 0.101 MPa to 492 K at 2.2 MPa. Thus, the degrees of superheat reduce from 123 K at 0.101 MPa to 4 K at 2.2 MPa. Therefore, there is less superheat to drive bubble growth at higher pressures.

We have also examined the pressure dependence of the “bubble-growth threshold” which is defined as the threshold surface temperature for the occurrence of the drop of the front-side reflectance signal at minimum fluence, namely, the

first appearance of bubbles causing Mie scattering. At the bubble-growth threshold of each ambient pressure the peak surface temperature is measured and plotted in Fig. 4. The solid line indicates the saturation curve and the dashed line the limit of superheat.¹¹ The area between the saturation curve and the limit of superheat curve is the region of metastable states. The actual superheat in the experiment is the temperature difference between the saturation curve and the bubble growth threshold.¹² The spontaneous growth of bubbles is known to depend on the radius of critical bubble and cavity centers on the solid surface. By assuming that the formation of critical nuclei causes the transition from Rayleigh scattering to Mie scattering, the radius of the nucleus can be estimated by the scattering transition size $R_{tr} \equiv \lambda/2\pi n$. Therefore, the radius of the critical nucleus is of the order of 0.06 μm . It is worth noting that this estimate is comparable to the thermal diffusion length in the liquid, which is 0.1 μm for water at 373 K. This agreement implies that the rate of heat diffusion into a liquid is a limiting factor for the onset of bubble growth in nanosecond time scale.

We have investigated the thermodynamics of phase transitions of liquids on the solid surface that is heated by a nanosecond laser pulse. Using a novel photothermal reflectance technique, we have found that nucleation begins as the surface reaches the boiling temperature but bubble growth is not initiated until higher surface temperature is attained. The bubble growth threshold requires the surface temperature to be up to 100 °C higher than the boiling temperature.

Support of this work by the National Science Foundation under Grant CTS-9317708 is gratefully acknowledged. The experimental work described in this letter has been performed at the IBM Almaden Research Center. The authors thank Xiang Zhang and Xianfan Xu at the University of California at Berkeley for the sample fabrication and the ellipsometric measurement of the sample optical properties.

¹H. K. Park, C. P. Grigoropoulos, W. P. Leung, and A. C. Tam, IEEE Trans. Compon. Packag. Manuf. Technol. A **17**, 631 (1994).

²A. Vogel, P. Schweiger, A. Frieser, M. N. Asiyu, and R. Birngber, IEEE J. Quantum. Electron. **26**, 2240 (1990).

³O. Yavas, P. Leiderer, H. K. Park, C. P. Grigoropoulos, C. C. Poon, W. P. Leung, N. Do, and A. C. Tam, Phys. Rev. Lett. **70**, 1830 (1993).

⁴L. A. Lompré, J. M. Liu, H. Kurz, and N. Bloembergen, Appl. Phys. Lett. **43**, 168 (1983).

⁵G. E. Jellison, Jr., D. H. Lowndes, D. N. Mashburn, and R. F. Wood, Phys. Rev. B **34**, 2407 (1986).

⁶H. K. Park, X. Xu, C. P. Grigoropoulos, N. Do, L. Klees, P. T. Leung, and A. C. Tam, Trans. ASME J. Heat Trans. **115**, 178 (1993).

⁷H. K. Park, Ph. D. dissertation, University of California at Berkeley, 1994.

⁸M. M. Martynyuk, Sov. Phys. Tech. Phys. **19**, 793 (1974).

⁹W. Fucke and U. Seydel, High Temp.-High Pressures **12**, 419 (1980).

¹⁰O. Yavas, P. Leiderer, H. K. Park, C. P. Grigoropoulos, C. C. Poon, W. P. Leung, N. Do, and A. C. Tam, Appl. Phys. A **58**, 407 (1994).

¹¹C. T. Avedisian, J. Phys. Chem. Ref. Data **14**, 695 (1985).

¹²V. P. Carey, *Liquid-Vapor Phase-Change Phenomena* (Hemisphere, Washington, DC, 1992).